

POLYMER PIPES IN TRENCHLESS APPLICATIONS: HDPE PIPE RESPONSE DURING PULLED IN PLACE INSTALLATION

A. G. Chehab and I. D. Moore

GeoEngineering Centre at Queen's –RMC, Queen's University, Kingston, Ontario, Canada

ABSTRACT

Constitutive models are presented for calculating HDPE pipe response during pulled in place installation. A soil-pipe interaction model is then presented to permit pulling forces to be estimated during pipe installation, and subsequently over the design life of these installations. The model includes consideration of the curved drill path during directional drilling, the shear stresses between soil and pipe during bursting and drilling, and the cyclic axial pulling forces that occur as each separate rod is recovered by the construction crew during pipe installation. The model calculates the distribution of axial forces along the pipes during and after installation, and includes consideration of the viscoelastic and/or viscoplastic strain recovery or stress relaxation once the pipe is attached at its end points (to valves or other appurtenances). Design adequacy is considered through comparisons of calculated axial forces to tensile stress limits for HDPE.

1. INTRODUCTION

Horizontal directional drilling and pipe bursting are two Trenchless Technologies used with increasing frequency to install polymer pipes without the costs and disruption associated with conventional 'cut and cover' installations.

'Horizontal directional drilling (HDD) is a technique for installing pipes or utility lines below ground using a surface-monitored drilling rig that launches and places a drill string at a shallow angle to the surface and has tracking and steering capabilities' (ASTM F 1962-99). A typical directional drilling operation involves three stages. First, a borehole is drilled along the desired path of the pipe. The cavity is then enlarged using single or multiple reaming. Finally, the new pipe is pulled into place. The cavity is stabilized through the processes using drilling mud.

During pipe bursting, a conical bursting head is pulled through an existing pipe, breaking it, enlarging the cavity, and pulling a replacement pipe into place.

At the end of the pulling process in both pipe bursting and horizontal directional drilling, the pipe is released from the rig and left to recover for a short time period. Finally the pipe is attached to existing infrastructure (such as manholes or hydrants) and placed into service.

These techniques developed by industrial innovators feature complex soil and pipe response which is not well understood. The success of these operations depends on knowledge of the pulling forces applied, the level of ground disturbance (and damage to adjacent infrastructure) during cavity creation, expansion or ground fracture from mud pressure, and the effect of the pulling operations and axial tensions on the pipes. Tensile stresses in the pipe vary with time during and after installation, and along the pipe. This applies especially to polymer pipes since viscoelastic strain recovery is prevented once the pipe is attached to its supply and termination points. The axial stresses during insertion and those that occur over the service life of the new pipe may influence the performance of the pipe selected.

2. INSTALLATION LOADS

2.1 Load components

During installation, the pipe interacts with the borehole and the drilling mud. If a straight segment is considered (Figure 1), the main applied forces are due to gravity, friction between the pipe and the ground surface or the borehole wall, and viscous drag from the drilling mud.

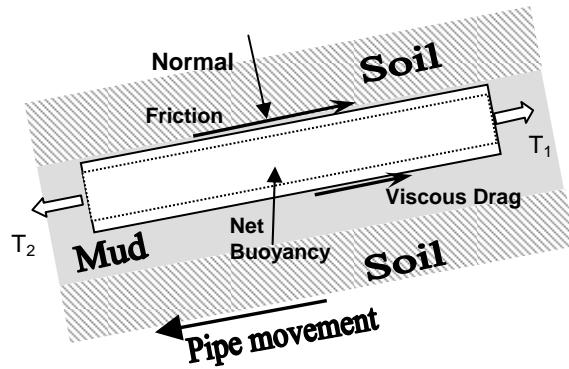


Figure 1. Installation forces on a straight pipe segment

2.2 Gravity Forces

The gravity force is usually the net buoyancy resulting from submerging the pipe in the drilling mud. For inclined segments, the net gravity or buoyancy force component along the pipe axis contributes to the total tensile force applied to the pipe, while the component normal to the pipe axis contributes to the normal force producing friction between the segment and the soil. The contribution of the gravity force $\Delta P_{\text{gravity}}$ per unit length is given by:

$$\Delta P_{\text{gravity}} = \frac{\pi}{4} (\gamma_{\text{mud}} \cdot OD^2 - \gamma_{\text{pipe}} (OD^2 - ID^2)) \cdot \sin \beta \quad [1]$$

where OD and ID are the external and internal diameters of the pipe, γ is the unit weight, and β is the inclination angle of the element under consideration. The first term in the equation accounts for buoyancy, whereas the second term accounts for the pipe weight. For installation where no mud is used, γ_{mud} can be set equal to zero.

2.3 Frictional forces

Forces also develop due to friction between the pipe and the borehole wall or the ground surface (for segments not yet in the borehole). While gravity forces may act with or against the pipe movement direction, frictional forces always act against the pipe movement. Adhesion may also contribute in some cases. The maximum shear force that can be mobilized per unit length is given by:

$$\text{Max.Shear} = a \cdot A_{\text{contact}} + \tan \delta \cdot N \quad [2]$$

where a is the adhesion, A_{contact} is the contact area per unit length, and $\tan \delta$ is the coefficient of friction between the pipe and the borehole wall (δ_{bore}) or ground surface (δ_{grond}). For a straight element, the normal force per unit length N is given by:

$$N = \frac{\pi}{4} (\gamma_{\text{mud}} \cdot OD^2 - \gamma_{\text{pipe}} (OD^2 - ID^2)) \cdot \cos \beta \quad [3]$$

2.4 Drag forces

Fluid drag is the shear force applied on the outer surface of the pipe being installed as a result of the movement of the viscous drilling mud relative to the pipe. The drilling fluid is usually pumped continuously during the drilling, reaming and pullback processes. Even if no fluid is pumped during pullback, any advance of the pipe through the mud confined in the borehole will cause the displaced mud to flow out of bore, i.e. past the pipe and/or the drilling string. That relative movement will still cause some drag forces on the pipe.

Fluid drag depends mainly on the properties of the slurry (drilling fluid containing soil cuttings), the annulus opening geometry and configuration (pipe and borehole size and eccentricity), and the rate of flow of slurry relative to pipe (pumping rate and pipe advance speed).

For a Newtonian fluid with viscosity μ , flowing in a concentric annulus, the drag shear stress τ_p and the mud drag force per unit length ΔP_{drag} are given by:

$$\tau_p = \frac{1}{4} \frac{dp}{dl} \left[\frac{R_{bh}^2 - R_p^2}{R_p \ln(R_{bh}/R_p)} - 2R_p \right] + \frac{\mu V_p}{R_p \ln(R_{bh}/R_p)} \quad [4]$$

$$\Delta P_{\text{drag}} = 2\pi R_p \tau_p \quad [5]$$

where R_{bh} and R_p are the radii of the borehole and pipe respectively, and V_p is the pipe movement speed. The pressure gradient dp/dl can be determined from the flow rate Q of the drilling mud in the borehole annulus using:

$$Q = \frac{\pi}{8\mu} \left(\frac{dp}{dl} \right) \left[R_{bh}^4 - R_p^4 - \frac{(R_{bh}^2 - R_p^2)^2}{\ln(R_{bh}/R_p)} \right] + \pi V_p \left[R_p^2 - \frac{R_{bh}^2 - R_p^2}{2 \ln(R_{bh}/R_p)} \right] \quad [6]$$

For an eccentric annulus, a modification factor that is a function of eccentricity can be applied to the calculated pressure loss (Haciislamoglu and Langlinas, 1990).

2.5 Curves

2.5.1 Force Components at Curves

Pulling a pipe segment through a curve not only causes bending stresses, but also magnifies the tensile force required to pull the segment. This is due to the additional normal force resulting when the pipe is forced to conform to the curve (due to bending stiffness) as well as the associated friction (the 'capstan' effect, explained below).

2.5.2 Capstan Effect

When a flexible pipe is pulled around a curve, "extra" normal force is created as a result of the change in the direction of the pulling force applied on the curved surface being considered, and friction between that curved surface and the pipe. The extra normal force can be calculated as:

$$N_{\text{curve}} \approx T.d\beta \quad [7]$$

where $d\beta$ is the change in direction along the element under consideration. To account for the curve effect, N_{curve} is added to N in Equation 2.

2.5.3 Pipe Bending/Stiffness Effect

Bending stresses and additional normal forces develop in the pipe segment when it is forced to conform to a horizontal or vertical curve. The tighter the radius of curvature, the higher the stresses and the normal forces that result. The additional normal forces lead to higher frictional forces and increased pulling forces.

For large diameter steel pipes, bending stresses and additional normal forces can be significant and should be considered. For polyethylene (PE) pipe, the safe curve radii are usually dictated by the drilling rod capacity, since they are stiffer than PE pipes and are subject to cyclic bending stresses as the curved drill string rotates. Research studies indicate that contributions from bending stiffness of PE pipes to increases in pulling force are insignificant over well designed curves. For example, Dareing and Ahlers (1991) analyzed the pullout force needed to remove drill strings from high curvature well bores, and concluded that the weighted cable or string model (that assumes zero flexural stiffness EI) provides a reasonable approximation of the pulling load, provided there are no severe local curves.

3. MODELLING PIPE MOVEMENT

The movement of every segment of the pipe is associated with the movement of the pulling head, which depends on several factors such as the rig size, pulling speed, length of each pulling rod, and time required to remove pulled rods. As previously stated, the pulling stage is usually carried out in steps, Figure 2. In each step, the pipe head is pulled with a constant speed for a distance usually equal to or twice the length of a single drilling rod. The pulling then stops for several seconds to remove the drill rod that was recovered. The movement of the head is represented by a stepped ramp function:

$$\text{Move}(t) = \begin{cases} \text{NPC} \times \text{PL} + (\text{PL}/\text{TP})t_c & t_c < \text{TP} \\ (\text{NPC} + 1) \times \text{PL} & \text{TP} < t_c < \text{TP} + \text{TR} \end{cases} \quad [8]$$

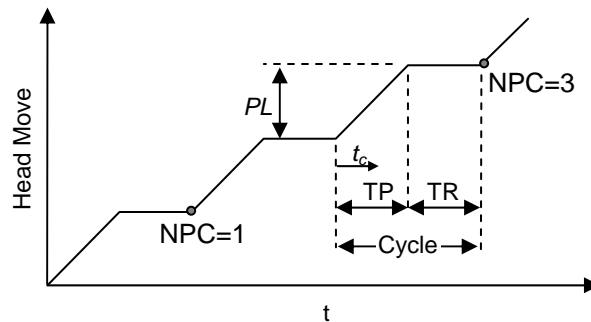


Figure 2. Time history of pipe head movement

Now, PL is the length pulled per cycle, TP and TR are the pulling time and rest time in each cycle, t is the time measured from the beginning of the process, and t_c is the time measured from the beginning of each cycle.

4. PIPE MATERIAL'S BEHAVIOUR

The mechanical properties of high density polyethylene are highly time and rate dependent and its response can differ significantly when subjected to different loading conditions. The constitutive behaviour of HDPE consists of an instantaneous elastic component, and time dependent viscoelastic and viscoplastic components. There is no well-defined yielding point beyond which plastic behaviour is experienced. Permanent viscoplastic deformation initiates at relatively low stresses and become significant at high stresses.

The model developed for this study combines, in series, an elastic (e) sub-model, a viscoelastic (ve) sub-model, and a viscoplastic (vp) sub-model, as shown in Figure 3.

$$\varepsilon(t) = \varepsilon_e(t) + \varepsilon_{ve}(t) + \varepsilon_{vp}(t) \quad [9]$$

The elastic sub-model is simply a spring that represents the instantaneous response of the material $\varepsilon_e(t)$:

$$\varepsilon_e(t) = \frac{\sigma(t)}{E_o} \quad [10]$$

where $\sigma(t)$ is the true stress and E_o is the modulus of the elastic spring. The viscoelastic sub-model can be mechanically represented, as described by Moore and Hu (1996), by a combination of nine Kelvin elements in series. The viscoelastic constitutive relation for an i th element can be written as:

$$\sigma(t) = E_i \varepsilon_i(t) + \eta_i \dot{\varepsilon}_i(t) \quad [11a]$$

where E_i , η_i , and $\varepsilon_i(t)$ are the elasticity and viscosity constants and strain of the Kelvin element, respectively. The total viscoelastic strain ε_{ve} is:

$$\varepsilon_{ve}(t) = \sum_{i=1}^9 \varepsilon_i(t) \quad [11b]$$

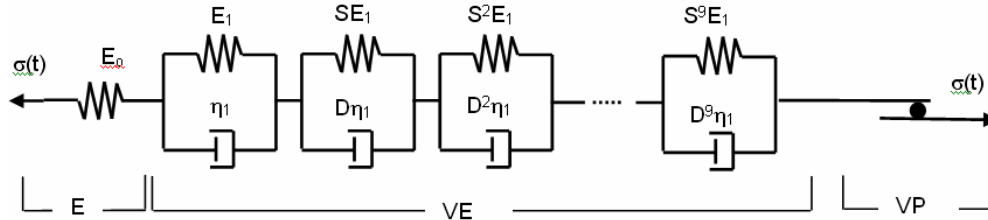


Figure 3: the Viscoelastic-viscoplastic material model used in the study (Chehab and Moore, 2004).

The viscoplastic submodel relates the viscoplastic strain rates $\dot{\varepsilon}_{vp}$ to both the stress level and the viscoplastic work (to account for the effect of the loading history) as shown in the equations below:

$$\dot{\varepsilon}_{vp} = C \cdot \left[\sigma \times \left(\alpha + \sqrt{\beta / (\gamma + w_{vp})} \right) \right]^n \quad n \geq 1 \quad [12]$$

where C is a scalar constant, α , β , and γ are model parameters that are usually strain rate dependents, and w_{vp} is the viscoplastic work per unit volume, given by:

$$w_{vp} = \int \sigma \cdot d\varepsilon_{vp} \quad [13]$$

Chehab and Moore (2004) derived the model parameters using the results of uniaxial compression tests conducted by Zhang and Moore (1997) at different engineering strain rates.

Table 1: Parameters of the constitutive model

Elastic Sub-model	Visco-elastic Sub-model	Elastic Sub-model
$E_0 = 1400 \text{ MPa}$	$E_1 = 3615.5 \text{ MPa}$ $\eta_1 = 43459.2 \text{ MPa}\cdot\text{s}$ $S = 0.845$ $D = 10.0$	$C = 0.01$ $n = 8$ $\alpha = 0.04581 \dot{\varepsilon}_{vp}^{0.0755}$ $\beta = 8.225 \times 10^{-5} \dot{\varepsilon}_{vp}^{0.0716} \text{ MPa}$ $\gamma = 0.001 \text{ MPa}$

The predictions of the material model for two load controlled tests are shown in Figure 4. Two HDPE samples were subjected to constant rate of loading, and then unloading at the same rate. The ability of the constitutive model to capture the loading and partial unloading response of the material is evident.

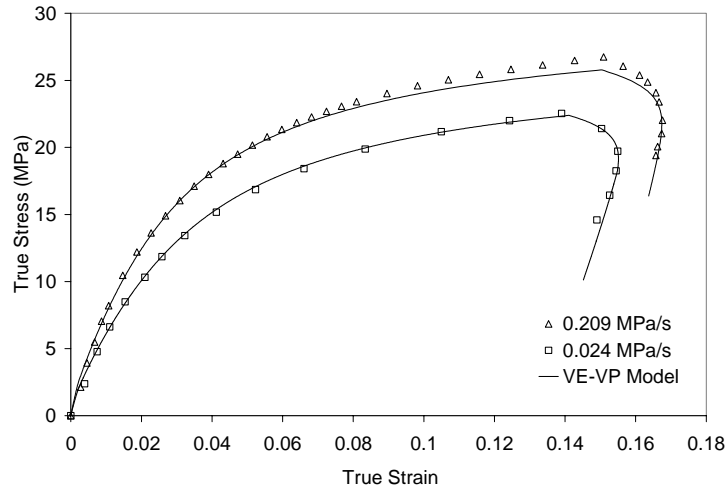


Figure 4: Performance of the material model (from Chehab and Moore, 2004)
Symbols: Experimental data – Line: Model

5. PIPE-SOIL INTERACTION:

The interaction between the pipe and the soil (borehole or ground surface) is assumed to exhibit the elastoplastic behaviour shown in Figure 5. The relative movement between the pipe and the surrounding soil is accompanied by linear increase in the interaction shear. This increase continues until the full shear limit given by Equation 2 is mobilized. Further relative displacement takes place as slippage at a constant shear force. Switching the direction of the relative movement will decrease the shear force linearly with a slope equal to K .

The slope K depends on several factors including the soil properties (modulus and Poisson's ratio), soil-mud cake, borehole geometry, borehole depth, and bedrock depth.

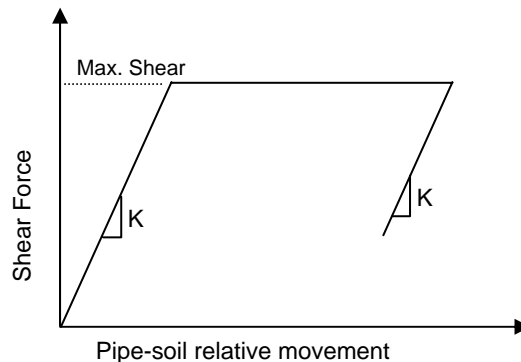


Figure 5. Assumed pipe-soil shear interaction mechanism

6. VALIDATION, RESULTS AND DISCUSSIONS

To evaluate the new model, denoted 'HDDPipe' in subsequent discussions, load calculations are first compared to those from well established and widely used methods. The model was used to compute the tensile forces along a steel pipe during a horizontal directional drilling installation reported by Baumert and Allouche (2002).

A 1275 m long crossing to a depth of 50 m of a large diameter (610 mm) steel pipe was considered (Figure 6). The borehole profile consists of three segments, a -10° entry segment, horizontal intermediate segment and a $+10^\circ$ exit segment. Two curves of 750 m radius provide the transitions between the segments.

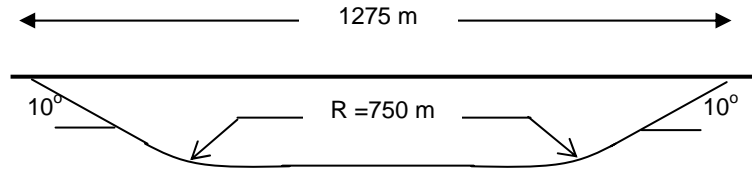


Figure 6. Profile of the crossing analyzed by Baumert et al. (2002).

Baumert and Allouche (2002) used the Driscopipe (1993), Drillpath (1996), and PRCI (Huey et al. 1996) methods to evaluate the pulling force along the profile for three sets of parameters representing upper bound values, lower bound, and intermediate or average values. The upper and lower bound parameters are given in Table 2.

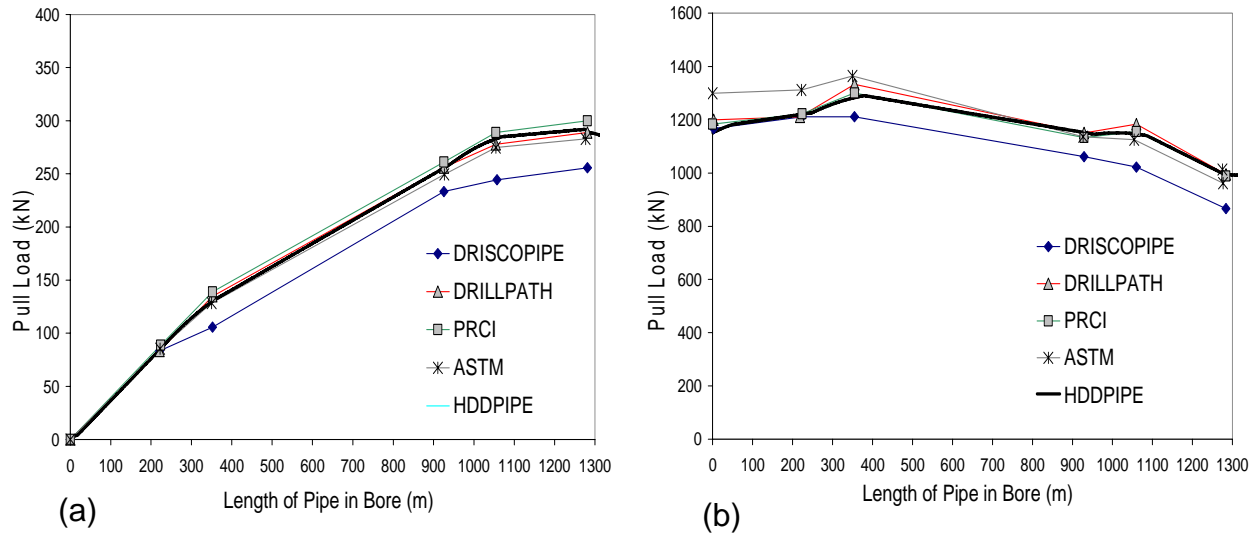
Table 2. Characteristics of tested soils.

	$\tan\delta_{\text{surface}}$	$\tan\delta_{\text{bore}}$	γ_{mud} (kN/m ³)
Low parameter set	0.0	0.21	10.0
High parameter set	0.5	0.3	14.4

Figures 7a and 7b show the calculations of Baumert and Allouche (2002) for upper and lower bound parameters, as well as calculations from the new model presented here (assuming zero adhesion). The predictions of the ASTM formulae (ASTM F 1962 – 99) are also shown. Neither adhesion nor mud drag are not considered in these calculations.

The results obtained using the model developed in this study agree well with those of the Drillpath and PRCI methods. All the methods produce load per unit length in linear segments. The differences are mainly at curves, where the Driscopipe method always predicts lower pulling loads since it does not account for load magnification due to the Capstan effect at curves.

The plots in Figure 7 provide general estimates of the pulling loads along the pipe. Of considerable interest to the authors, however, is the nature of load changes during installation including the time periods when the rods are being removed, e.g. Baumert et al. (2004), and how these load changes are affected by the stiffness of the pipe and the surrounding soil. For that purpose, another problem is now examined.



(a) Lower bound (b) Upper bound
Figure 7. Pulling load versus pulled length

A high density polyethylene pipe with 400 mm outer diameter and 10 mm wall thickness is installed underground using horizontal directional drilling. The borepath profile is shown in Figure 8. The ground surface at the pipe entry point is assumed horizontal and length of pipe in contact with the ground surface is 50 m. The coefficients of friction of the pipe with ground surface and borehole are 0.3 and 0.4 respectively. The interaction stiffness K is assumed to be 1 MN/m per meter of borehole length. Drilling mud that has specific gravity of 1.5, yield shear strength of 32 Pa, and viscosity of 2.1×10^{-2} Pa.s, is continuously pumped during pullback at a rate of 20 L/s. The Viscoelastic-viscoplastic constitutive model defined above is used to model the mechanical response of the pipe during and after installation.

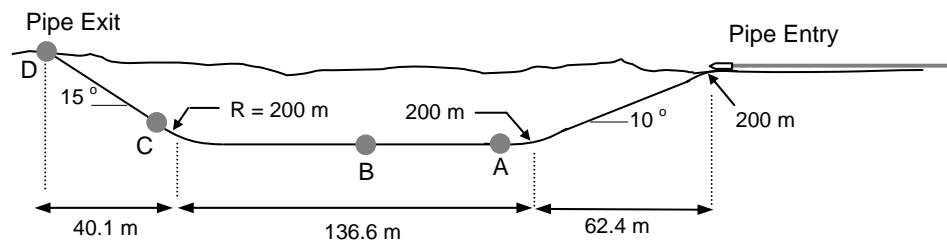


Figure 8. The borehole profile of the problem considered.

The pullback process is performed in steps. Each step involves pulling two drilling rods in 22 seconds, then pausing for 30 seconds to allow removal of the pulled rods. The combined length of the two rods is about 10.5 m. To account for elastic and viscoelastic recovery and possible thermal contraction, an extra 8 m (representing about 3 % of the pipe length) is pulled out of the pipe exit point. The pipe is then left for 1 hour to recover before fixing both ends to existing infrastructure.

Table 3 demonstrates the change of the tensile stress at selected locations after installation is complete. The specific locations that have been considered are marked on Figure 8. Point B is nearly to the middle of the pull, and point D is at the pipe head (or nose). Once released, the stress drops to zero at the pipe head. Other locations along the pipe experience varying levels of tensile stress decrease. The tensile stress continues to drop with time after the pipe ends are fixed to rigid appurtenances as shown in the table.

The rate of change in the tensile stress varies along the pipe and with time as it is influenced by a complex combination of phenomena, including stress relaxation, restrained recovery, and interaction with the surrounding soil. Points A and B in the rear half of the pipe experience stresses that decrease monotonically with time from the completion of installation

(the end of pullback). Point D where the pipe is attached to the drill string is subjected to the largest axial pulling stresses, but axial tensions drop to zero when this end is released and the pipe is allowed to undergo a period of axial shortening (length recovery). However, the stress at this location ultimately becomes compressive, since the rest of the pipe remains under axial tension, and the 'zero length change' condition imposed once the ends are fixed to appurtenances leads to compression in this least tensile segment of the pipe. Stress histories of this kind during and after installation are being investigated, to understand the likelihood of ring fracture under sustained axial tension over the service life of the pipe.

Table 3: Change of tensile stress with time at different locations on the pipe

Stage	Tensile Stress (MPa) at Selected Locations on the Pipe			
	A	B	C	D
End of Pullback	3.357	4.158	7.719	7.923
After instant recovery	3.328	3.660	0.497	0
5 minutes recovery	2.944	3.468	0.505	0
End of release - Fixing	2.392	2.865	0.506	0
One hour after fixing	2.276	2.737	0.509	0
7.5 hours after fixing	2.057	2.488	0.355	-0.127

7. CONCLUSION

A new model has been developed to calculate tensile force and axial stress over the length of HDPE pipes during and after pulled in place pipe installation, using the history of pipe movement during installation. Gravity forces, pipe-soil interaction forces, and viscous drag force due to mud flow past the pipe are considered. The model accounts for pipe-soil interaction, employing a simple model accounting for adhesion, friction, and stiffness of the soil medium. Most importantly, the effect of the nonlinear time dependent behaviour of the high density polyethylene on the pipe performance is accounted for by employing a complex constitutive model that considers elastic, viscoelastic, and viscoplastic response.

The performance of the model in predicting installation loads was evaluated through comparisons to calculations from established methods. A further example problem demonstrated that the model provides details of stress history, during and after installation, at various locations along the pipe, accounting for the nonlinear, time dependent polymer behaviour (cyclic loading during installation, length recovery immediately after installation, and zones of tensile and compressive axial stresses as pipe length is fixed over the service life of the structure). The model has the flexibility to account for different installation procedures, including the pulling speed, length of installation rod, rest period of each pulling cycle, and time period during which length recovery is permitted after installation.

8. ACKNOWLEDGEMENT

This work is part of a Strategic Research project funded by the Natural Sciences and Engineering Research Council of Canada. Dr Moore's position at Queen's University is supported by the Canada Research Chairs program.

9. REFERENCES

- ASTM International, Designation: F 1962 – 99, Standard guide for use of maxi-horizontal directional drilling for placement polyethylene pipe or conduit under obstacles, including river crossings, 1-17
- Baumert, M.E. and Allouche, E.N. 2002. Methods for estimating pipe pullback loads for horizontal directional drilling (HDD) crossings, *Journal of Infrastructure Systems*, ASCE, 8(1): 12-19.
- Baumert, M.E., Allouche, E.N., and Moore I.D. 2004. Experimental investigation of pull loads and borehole pressures during horizontal directional drilling installations, *Canadian Geotechnical Journal*, ASCE, 41: 672-685.
- Dareing, D.W. and Ahlers, C.A. 1991. Tubular bending and pull-out forces in high curvature well bores, *Journal of Energy Recourses Technology*, 113: 133-139.
- Drillpath™, 1996. Theory and user's manual, Infracore L. L. C., Houston, Texas, USA.

The First Pan American Geosynthetics Conference & Exhibition
2-5 March 2008, Cancun, Mexico

- Driscopipe® 1993. Technical expertise application of driscopipe® in directional drilling and river-crossings, *Technical Note #. 41*.
- Huey, D.P., Hair, J.D. and McLeod K.B. 1996. Installation loading and stress analysis involved with pipelines installed in horizontal directional drilling, *Proceedings of the No-Dig Conference – New Orleans, North American Society for Trenchless Technology*.
- Haciislamoglu, M. and Langlinais, J. 1990. Non-Newtonian flow in eccentric annuli, *Journal of Energy Resources Technology*, 112(3): 163-169.
- Zhang, C. and Moore, I.D. 1997. Nonlinear mechanical response of high density polyethylene. Part II: Uniaxial constitutive modeling, *Polymer Engineering and Science*, 37(2): 414-420.